

---

# TokenLearner: What Can 8 Learned Tokens Do for Images and Videos?

---

Michael S. Ryoo<sup>1,2</sup>, AJ Piergiovanni<sup>1</sup>, Anurag Arnab<sup>1</sup>, Mostafa Dehghani<sup>1</sup>, Anelia Angelova<sup>1</sup>

<sup>1</sup>Google Research

<sup>2</sup>Stony Brook University

{mryoo, ajpiergi, aarnab, dehghani, anelia}@google.com

## Abstract

In this paper, we introduce a novel visual representation learning which relies on a handful of adaptively learned tokens, and which is applicable to both image and video understanding tasks. Instead of relying on hand-designed splitting strategies to obtain visual tokens and processing a large number of densely sampled patches for attention, our approach learns to mine important tokens in visual data. This results in efficiently and effectively finding a few important visual tokens and enables modeling of pairwise attention between such tokens, over a longer temporal horizon for videos, or the spatial content in images. Our experiments demonstrate strong performance on several challenging benchmarks for both image and video recognition tasks. Importantly, due to our tokens being adaptive, we accomplish competitive results at significantly reduced compute amount.

## 1 Introduction

Images and videos provide an abundance of visual information. Image understanding is a long standing problem in computer vision, and despite incredible advances, obtaining the best visual representation for a variety of image understanding tasks is still an active area of research. Videos, in addition to addressing a similar image understanding task, require employing effective spatial-temporal processing of both RGB and time streams to capture long-range interactions [5, 36, 21, 17, 23, 12, 33, 20, 24, 1]. An important aspect of this understanding is how to quickly learn which parts of the input video stream are important, both spatially and temporally, and to focus computational resources on them. But what basic processing mechanism are able to do so successfully for both videos and images?

Recent advancements in image understanding demonstrate improved accuracy on vision classification tasks. For example, departing from standard convolutional approaches, the Vision Transformer (ViT) [9] treats the image as a sequence of patches, utilizing the Transformer architecture [38] similar to text understanding.

Standard approaches for video recognition take videos as stacked images (i.e., a space-time volume) and tend to extend 2D neural architectures to 3D (e.g., 3D-ResNets [17, 5, 37, 11]). In parallel to the Vision Transformer for images, some approaches [2, 3] proposed to create 3D ‘cubelet’ video tokens on a regular 3D-grid which are further processed by a Transformer, resulting in computationally heavy models. There are too many tokens to process, especially for longer videos.

The main question addressed in this work is how to adaptively learn the representation from visual inputs to most effectively capture the spatial information for images and spatio-temporal interactions for videos. Here are our main ideas:

The first key observation is we are able to learn to represent visual data by adaptively learning the tokens from the input. This is in contrast to previous approaches which densely sampled tokens e.g. 16x16 or 32x32 for either images or videos [9, 3].

Specifically, we can learn to compute the important tokens from the input only, so that the tokens become adaptive to the input data. More specifically, we compute multiple spatial weight maps per frame with a spatial attention mechanism. The goal of these maps is to learn which areas are of importance. Here, each spatial weight map is multiplied with the input to form a ‘token’, to be processed by the subsequent learning modules.

Furthermore, we find that very few tokens may be sufficient for a visual understanding task. More specifically, for video recognition we show improved performance over the state-of-the-art on two challenging datasets using only 8 tokens per frame. For images we show that one can significantly reduce the computational budget of the Vision Transformer, when inserting 8-16 tokens as an intermediate representation (instead of keep 200~500), thus reducing the number of total FLOPS by half.

The approach is simple, efficient, and, as shown by the results, outperforms methods including both convolutional methods and previous space-time Transformer ones from prior art.

## 2 Adaptive Tokenization in Images and Videos

In Vision Transformer architectures such as ViT [9], an input image is first tokenized by splitting it into small (e.g., 16x16) spatial patches, which are used as input to the model. Similarly, in recent video Transformer architectures, such as ViViT [2] and TimeSformer [3], the video is tokenized by cutting the video into 2d spatial or 3d spatio-temporal cubes on a regular grid.

Instead of processing fixed, tokenized inputs, our attention module learns the tokens that are to be used for the recognition task. We gain several important properties by doing so: (1) We enable the adaptive tokenization so that the tokens could be dynamically selected conditioned on the input. (2) This also effectively reduces the total number of tokens for the transformer, which is particularly beneficial considering that the computation is quadratic to the number of tokens (and that there are many tokens in videos). (3) Finally, we provide an ability for each subsequent layer learn to rely on different space-time tokenizations, potentially allowing different layers to capture different aspects of the video. These dynamically and adaptively generated tokens could be used in the standard transformer architectures such as ViT, or can be used together with specialized video components which we discuss further in Section 3.

### 2.1 TokenLearner

Let  $X$  be an input tensor with a space-time shape:  $X \in \mathbb{R}^{H \times W \times T \times C}$  where  $H \times W$  corresponds to the spatial dimension of the input,  $T$  is the temporal dimension (i.e., number of frames), and  $C$  is the number of channels. Let  $x^t$  be a temporal slice of it, corresponding to the frame  $t$ :  $x^t \in \mathbb{R}^{H \times W \times C}$ . In the case of an image input,  $T = 1$  and  $X = x^t$ . Note that  $X$  could also be an intermediate representation within a network, and  $x^t$  will be its slice in such case.

For every time frame  $t$ , we learn to generate a set of  $S$  tokens,  $Z^t = \{z_i^t\}_{i=1}^S$ , from the input frame  $x^t$ . Specifically, we formulate a tokenizer function,  $z_i = A_i(x)$ , which maps the input frame  $x$  to a token vector  $z_i: \mathbb{R}^{H \times W \times C} \mapsto \mathbb{R}^C$ . The idea is to learn our tokenizer function  $A_i$  to adaptively select an informative combination of pixels (or spatial locations) in  $x^t$ . This way, our tokens will not be fixed splits of the input tensor, but a set of adaptively changing spatial selections. Different tokens will be mined per frame, allowing us to model their space-time relations/interactions. We also set  $S$  to be smaller than  $H \times W$  (e.g.,  $S = 8$  and  $H \times W = 256 \times 256$ ), enabling the model to easily consider more frames temporally.

Here, our tokenizer  $z_i = A_i(x)$  is implemented with a spatial attention mechanism: i.e., the model learns to compute a weight map (of size  $H \times W$ ) conditioned on the input  $x$ . The attention map, which is a function of the input itself, is applied to the input to generate the token:

$$z_i = A_i(x) = W_i \odot x = \alpha_i(x) \odot x, \quad (1)$$

where  $\odot$  is the Hadamard product (i.e., element-wise multiplication) and  $\alpha_i(\cdot)$  is implemented with a single or multiple convolutional layers followed by a sigmoid function. It has a form of an element-

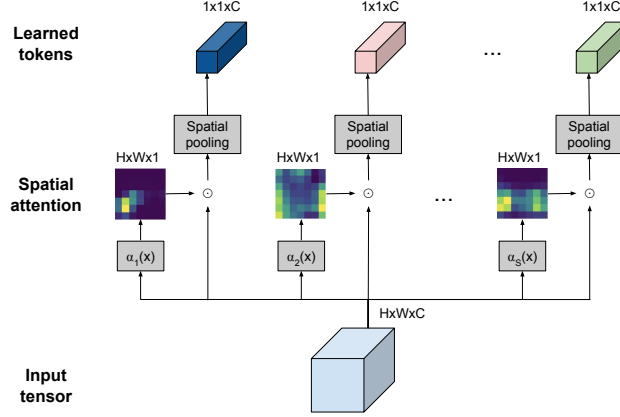


Figure 1: Visual illustration of the TokenLearner module, applied to a single image. TokenLearner learns to spatially attend over a subset of pixels, and generates a set of token vectors adaptive to the input. Note that the input to the TokenLearner module could also be intermediate tensors in a network.

wise spatial self-attention. Finally, spatial global average pooling is applied on top of them to reduce the dimensionality to  $\mathbb{R}^C$ .

We specifically name our token learning component as “TokenLearner”. Figure 1 visually summarizes the TokenLearner module. In the case of a video, the set of tokens are finally collected as:  $Z = \bigcup_t \{Z^t\}$ , combining a set of  $S$  tokens found for each frame.  $|Z| = ST$ .

### 3 Vector Transformer and TokenFuser for Videos

In this section, we further introduce components to better capture space-time interactions between the tokens in videos: Vector Transformer and TokenFuser. Although the TokenLearner itself could be applied to a video model without these components, we found Vector Transformer and TokenFuser to be particularly effective for videos when combined together with the TokenLearner.

Once TokenLearner generates adaptively learned tokens, a vector attention between key-query pairs is computed. This can be thought as a version of Transformer in which the number of heads is the same as channels, allowing us to learn a different attention matrix for each channel. It captures in an efficient way pairwise space-time relations per channel, particularly benefiting tokens with rich channel information (Sections 3.1). Finally, the transformed tokens are explicitly fused with a linear layer to capture the spatio-temporal patterns formed by the tokens (Section 3.2). This results in a lightweight convolution-free approach, which brings forth an efficient video representation by capturing long-range visual patterns.

Figure 2 provides an overview of the combined module for videos.

#### 3.1 Vector Transformer: Pairwise vector attention

Given  $Z$ , a set of tokens reflecting different space-time aspects of a video, we model space-time interactions between them with a Transformer mechanism [38]. We follow the formulation of [44], which enables a vector-version of the Transformer, although it is also possible to incorporate other attention mechanisms like multi-head and dot-product attention.

For every token  $z_i$ , the output of the Transformer  $y_i$  is computed by considering all possible  $z_j$  as:

$$y_i = \sum_{z_j \in Z} \gamma(f_q(z_i) \odot f_k(z_j)) \odot f_v(z_j) \quad (2)$$

where  $i$  and  $j$  are the indexes of the tokens in  $Z$  whose size is  $|Z| = ST$ .  $f_q$ ,  $f_k$ , and  $f_v$  are the linear layers projecting the tokens.  $\gamma$  is an extra projection layer to match the channel dimensionality

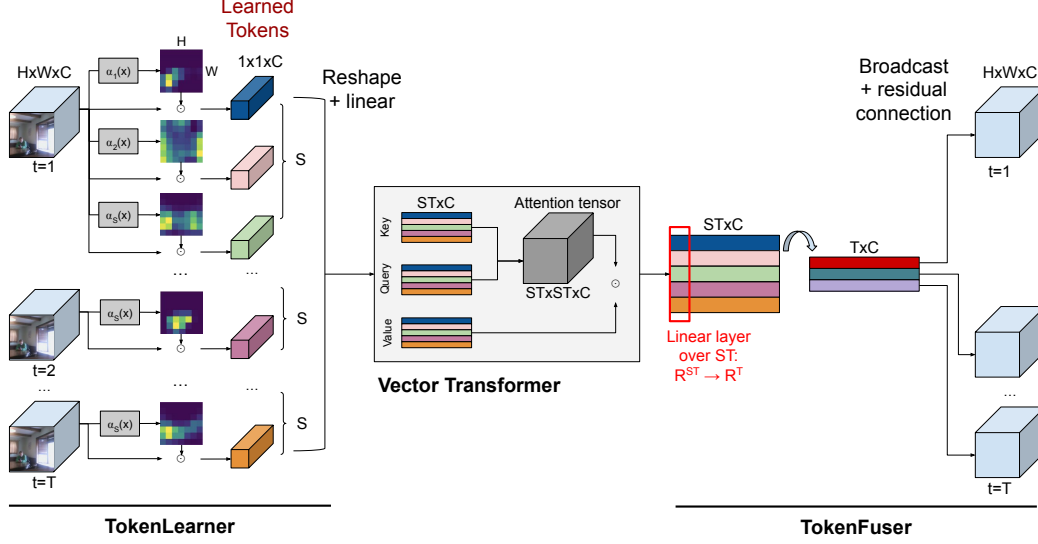


Figure 2: TokenLearner, vector Transformer, and TokenFuser combined for video representation. The TokenLearner first learns to generate a set of token vectors, the vector Transformer models their space-time relations, and TokenFuser combines them.  $S$  is the number of tokens we learn per frame, and  $T$  is the number of frames.  $C$  is the number of channels, which we made to be identical across the module for efficiency. Note that this combination can serve as a ‘module’ itself, and one may stack such module multiple times within the network.

followed by a softmax function over  $j$ . When the channel sizes of the projections are identical,  $\gamma$  is simplified as a single softmax layer identical to the standard transformer.

In the original transformer notation, the query matrix  $Q$  corresponds to our  $\{f_q(z_i)\}_i$ , and the key matrix  $K$  corresponds to our  $\{f_k(z_j)\}_j$ . Instead of computing the dot product between  $Q$  and  $K$  as  $QK^T$  to generate the attention ‘matrix’, this vector formulation computes an attention ‘tensor’  $\{\gamma(f_q(z_i) \odot f_k(z_j))\}_{(i,j)}$  preserving the channel information. It has shape  $ST \times ST \times d$  where  $d$  is the intermediate channel size. The computed attention tensor is multiplied with the value matrix  $\{f_v(z_j)\}_j$  to get the final transformer outputs.

Notice that this vector transformer is a global representation, and the temporal range of the information it is able to capture entirely depends on what tokens we provide to it. With our learnable adaptive tokens, we have the capability to cover a larger number of frames and focus on the temporal structure.

### 3.2 Token fusion and broadcasting

After TokenLearner generates the tokens and the Transformer learns their pairwise interactions, TokenFuser could be used to combine the tokens and information across our space-time tokens. This enables the model to capture spatio-temporal ‘patterns’ formulated by the tokens. Unlike the vanilla Transformer operation which learns to perform weighted summation of tokens based on pairwise relations, our TokenFuser component is designed to explicitly consider the patterns formulated by the space-time tokens.

Given a set of output tokens  $Y = \{y_i\}_i$ , we stack them to form a matrix of size  $\mathbb{R}^{ST \times C}$ , and apply a linear layer (i.e., a fully connected MLP layer) over the tokens, not channels. That is, we learn a linear function of  $\mathbb{R}^{ST} \mapsto \mathbb{R}^T$  where  $S$  is the number of our tokens mined per frame and  $T$  is temporal size of the input tensor, and apply it to every channel independently. If we denote each channel of  $y_i$  as  $y_i[c]$ , what we learn per frame  $t$  is a weighted summation of the tokens per channel:

$$o_t[c] = \sum_{y_i \in Y} w_i[c] \cdot y_i[c] \quad (3)$$

We believe this also has a connection to the observations from the concurrent work, MLP Mixer [35].

Once we have the vector representation computed per time step by combining tokens,  $o_t$ , we broadcast it to every spatial location (i.e., pixels) of the input tensor and add it with the residual connection from the input.

## 4 Experiments with Images

In order to validate the power of the TokenLearner module, we first try TokenLearner on image representation learning. This is done by inserting the TokenLearner within standard transformer models. Vector Transformer and TokenFuser are not used in these experiment, and we focus on evaluating the effectiveness of the TokenLearner itself.

### 4.1 Network architecture implementation

We use the Vision Transformer architecture [9], following its detailed settings and implementation. We particularly use ViT-B/16 as our backbone, while also applying the TokenLearner to ViT-B/32 (the same model but with an initial patch size of 32x32 in the beginning) and ViT-S/32 (smaller version with 384 channels). The backbone models have 12 transformer layers. The input resolution is 384x384 or 224x224 depending on the dataset (i.e., 576 or 196 tokens).

The main change is that now we insert TokenLearner in the middle of the network, such as after the 6th transformer among 12 (Figure 3). We also modified some of our models to have more transformer layers (e.g., 22 instead of 12), and we specify this when we do so.

We tried various number of tokens including  $S = 8, 16, 32$ , and use  $S = 8$  as our default setting. That is, the TokenLearner is learning to abstract an image into 8 tokens. The spatial attention function ( $\alpha$ ) in TokenLearner is implemented with three 3x3 conv. layers (with gelu in between), whose channel size is identical to the number of tokens (i.e.,  $S = 8$ ).

### 4.2 Image classification datasets

**ImageNet:** We use the popular image benchmark, ImageNet [7]. For our experiments, we use the standard ImageNet version which has 1000 categories and 1.1M images. We use the image resolution of 384x384.

**JFT-300M.** The JFT-300M dataset is an internal dataset collected for training image classification models, which was first introduced by [34]. Images are harvested from the web and are filtered to maximize label precision. It contains 300M images and has been shown to be suitable for learning high-capacity models, such as transformers.

In this work, we use the JFT-300M dataset only for pre-training purposes, following the evaluation protocol, previously established for ViT [9]. We use the image resolution of 224x224 for this.

### 4.3 Ablation: where should we have TokenLearner?

We first conducted an ablation to decide the best location to place the TokenLearner within the model. Figure 4 shows the results. It is showing the few-shot classification accuracies on ImageNet, following the protocol of ViT [9]. In addition, we show how the computation amount (FLOPS) changes per TokenLearner location. Basically, due to the large difference between the number of tokens with and without the TokenLearner (e.g., 8 with TokenLearner vs. 196 without), the computation of the transformers after the TokenLearner module becomes almost negligible compared to the transformers before the TokenLearner location.

We found that inserting TokenLearner in the middle of the network (at 1/2) achieves almost identical accuracies, while cutting the computation by (almost) half. In addition, having the TokenLearner at the later layer (after 3/4 of the network) achieves even superior performance compared to not using the TokenLearner while performing faster.

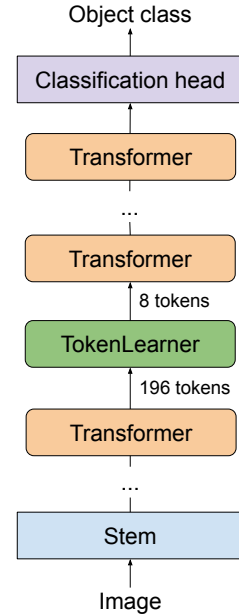


Figure 3: Our network following the ViT architecture. TokenLearner is inserted.

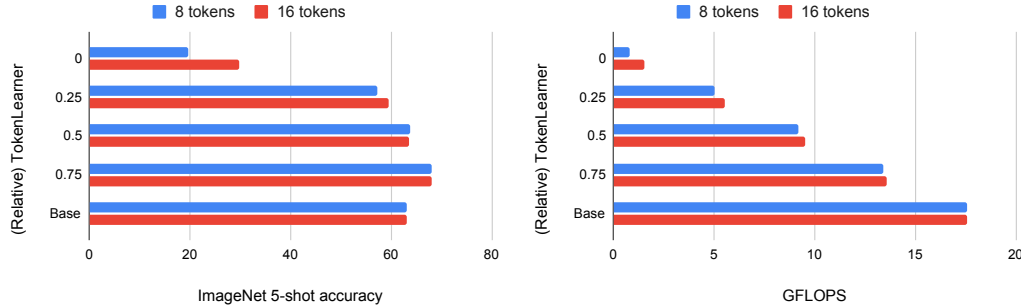


Figure 4: ImageNet 5-shot accuracy (left) and FLOPS (right) per different TokenLearner location within the model. ‘0’ means that the TokenLearner is at the very beginning of the model (before any transformer), ‘0.5’ means the middle of the model, and ‘Base’ means that there is no token learning.

#### 4.4 Results

Following the protocol established in ViT [9], we evaluated the models with and without TokenLearner in terms of (i) fine-tuning accuracies and (ii) few-shot accuracies. For the fine-tuning accuracies, we pre-train the model with JFT and fine-tune it with the original ImageNet dataset using an image resolution of 384x384 as done in [9]. For the few-shot accuracies, we also follow the protocol of ViT [9] where we do a regularized least-squares regression that maps the (frozen) representation of a subset of training images to  $\{-1, 1\}^K$  target vectors. We report 5-shot ImageNet Top-1 accuracy, as well as the 5-shot accuracies averaged over multiple datasets: Caltech101, Caltech-UCSD Birds 2011, Cars196, CIFAR100, colorectal\_histology, DTD, ImageNet, Oxford-IIIT Pet, and UC Merced Land Use Dataset. Few-shot accuracies are particularly interesting as it shows the generalization capability of the representation itself being learned. We note that 5-shot accuracy was also used to evaluate the representations learned by ViT [9]. In all these experiments, we inserted the TokenLearner module exactly at the mid-point of the network, using 8 tokens, which showed the best accuracy-speed balance from the ablation.

Figure 5 and Table 1 shows the ImageNet fine-tuning evaluation results. We show accuracies of various versions of ViT and their TokenLearner versions, as specified in Section 4.1. We are able to observe that there is a substantial improvement in efficiency-accuracy trade-offs.

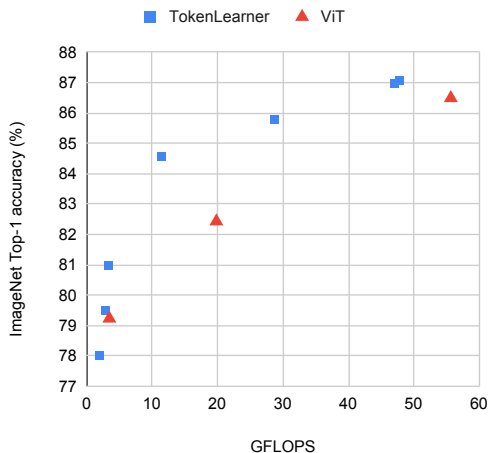


Table 1: ImageNet fine-tuning Top1 accuracies and FLOPS. The numbers in the parenthesis are the number of transformer layers. 16-TokenLearner is with 16 tokens instead of 8.

Method	GFLOPS	Accuracy
ViT S/32	3.4	79.23
ViT B/32	19.8	82.43
ViT B/16	55.6	86.49
TokenLearner S/32	1.9	78.0
TokenLearner B/16	28.7	85.79
TokenLearner S/32 (22)	3.3	80.97
TokenLearner B/32 (20)	11.5	84.57
TokenLearner B/16 (21)	47.1	86.98
16-TokenLearner B/16 (21)	47.7	87.07

Figure 5: Visualization of ImageNet fine-tuning accuracies of the baseline ViT models vs. TokenLearner. X-axis is GFLOPs, which measures the amount of computation required.

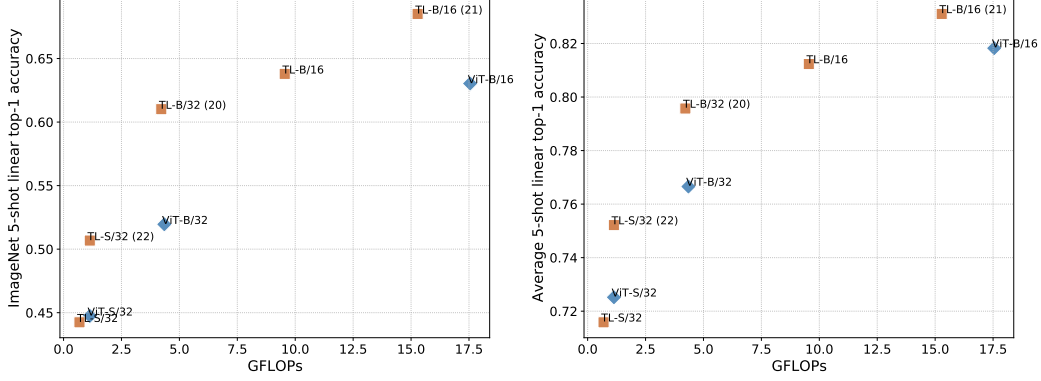


Figure 6: Few-shot classification experiments. It shows 5-shot classification accuracies on ImageNet (left) and average of multiple datasets listed in Sec. 4.4 (right). ‘TL’ stands for TokenLearner.

When directly applied to ViT (e.g., B/16), TokenLearner maintains the accuracy of ViT, while reducing the computation by almost a half. When more layers are used together with the TokenLearner, we are able to utilize the computation saved by the TokenLearner in the form of additional layers, and it performs superior while still having less FLOPs. The number of tokens the baseline ViT B/16 processes is 576, while the TokenLearner learns  $S = 8$  tokens. As a result, as mentioned in the above subsection, the computation of the transformers after the TokenLearner module becomes almost negligible compared to the transformers before the TokenLearner location.

Figure 6 shows few-shot experiment results. For these experiments, an image resolution of  $224 \times 224$  is used following [9]. The baseline ViT therefore uses 196 tokens (as opposed to 576 used in ImageNet fine-tuning experiments). This makes the gap between the number of tokens used in TokenLearner and ViT smaller (compared to fine-tuning setting), increasing TokenLearner’s relative accuracy. It is interesting to observe that the accuracies of TokenLearner does not drop (e.g., TokenLearner-B/16 vs. ViT-B/16), despite the difference in the number of tokens.

## 5 Experiments with Videos

### 5.1 Network architecture implementation

We follow the Bottleneck Transformer [32] network style, while taking advantage of X3D [11] as the backbone.

Specifically, we modified X3D to be more computationally efficient by (1) replacing its 3D XYT convolutional layers with a pair of 2D conv. layer and 1D conv. layer, and (2) removing Squeeze-and-Excitation layers [18] and swish activations. Our backbone could be viewed as  $X(2+1)D$ . We use the channel sizes and the number of layers identical to X3D-M, which is an efficient model.

Based on such  $X(2+1)D$  architecture, and following the Bottleneck Transformer concept, we replace the space-time convolution layers in the last block with our transformers. Figure 7 illustrates the residual module architecture, which is repeated multiple times in the block. We have tried different versions, and our final model is built by replacing 1D temporal convolution layer in the  $X(2+1)D$  modules. Compared to the use of the standard 1D conv., the TokenLearner actually has 3.1 less GFLOPs (as also shown in Table 5) in the 64 frame setting. The spatial attention function in TokenLearner is implemented with one conv2d layer.

We provide  $224 \times 224 \times 64$  videos for training and  $256 \times 256 \times 64$  videos for testing. After the 3rd residual block, the input tensor has shape  $8 \times 8 \times 64$ , and this becomes the input to the TokenLearner. For an efficient

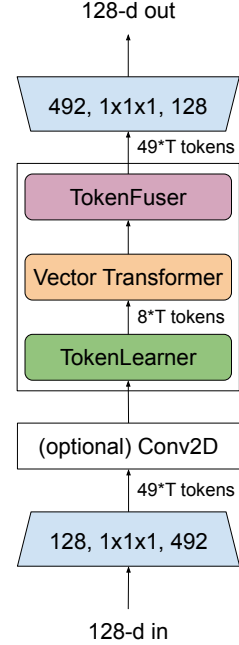


Figure 7: Our network module following the bottleneck transformer, with  $X(2+1)D$  backbone. It is an inverted bottleneck.

Table 2: Performance on the Charades multi-label classification task. 12 fps setting. Performance is measured using the Mean Average Precision (mAP) since more than one ground truth action is possible. Methods with RGB and optical flow input modalities are listed.

Method	Input	Pre-train	mAP
I3D [5]	RGB	Kinetics	32.9
I3D from [39]	RGB	Kinetics	35.5
I3D + Non-local [39]	RGB	Kinetics	37.5
EvaNet [25]	RGB	Kinetics	38.1
STRG [40]	RGB	Kinetics	39.7
LFB-101 [42]	RGB	Kinetics	42.5
SGFB-101 [19]	RGB	Kinetics	44.3
SlowFast-101 [12]	RGB+RGB	Kinetics	45.2
AssembleNet-50 [29]	RGB+Flow	None	47.0
Multiscale ViT [10]	RGB	Kinetics	47.7
AssembleNet-101 [29]	RGB+Flow	Kinetics	58.6
AssembleNet++ [28] (w/o object)	RGB+Flow	None	55.0
MoViNets [22]	RGB	None	63.2
Backbone (X(2+1)D-M)	RGB	None	62.7
Ours	RGB	None	<b>66.3</b>

implementation the intermediate channel size of TokenLearner was set identical to the output channel size,  $d = 432$ . Notice that 64 frames were used to best capture longer-term temporal information.  $S = 8$  number of tokens were used.

The training details are described in the Appendix.

### 5.1.1 Video recognition datasets

**Charades dataset:** The Charades dataset [30] is a dataset collected by assigning activity tasks which people in various environments are acting out, for example by performing a sequence of actions which involve interaction with objects. For example, sitting on the couch and reading a book, closing the book, standing up and speaking on the phone. It comprises 8000 training and 1686 validation videos with an average duration of 30 seconds. It has 157 activity classes. This dataset is very challenging as it is a multi-class, multi-label video dataset, that is, more than one activity can occur at the same time, and it includes fine grained motions or interactions with small objects in real-world environments. We follow the standard evaluation protocols, reporting the mean Average Precision (mAP) % (v1 classification setting of the dataset). We used the frame rate of 6 fps and 12 fps to obtain the training/testing videos (12 fps worked better). The dataset has a Non-Commercial Use license.

**AViD dataset:** The Anonymized Videos from Diverse countries (AViD) dataset [26] is a unique dataset which is representative of the world’s population video content generation. It is collected from videos uploaded from multiple countries across six continents and demonstrates higher diversity compared to other video datasets in its concepts, actions and visual representations. For example a ‘greeting’ in certain countries involves a handshake, in some a kiss, but in others a slight bow. The dataset is explicitly designed to contain less bias, encourage diversity, while respecting privacy and licenses. The AViD dataset contains 887 classes and 450k videos (410k training 40k testing) and is of comparable size to Kinetics-400 and Kinetics-600 datasets with 400 and 600 classes respectively, also containing variable duration videos 3 – 15s. We report classification accuracy over the 887 classes.

All the videos in the dataset have the Creative Commons License.

## 5.2 Results

**Charades dataset results:** In Table 2 we compare the proposed TokenLearner to the state-of-the-art methods. Our approach outperforms these, including recent work of which is most aligned to ours. The mAP of 66.3 % on Charades classification establishes the new state-of-the-art.



Table 3: Performance on the Anonymized Videos from Diverse countries (AViD) dataset. Performance in terms of mean accuracy is shown in % averaged over 887 classes. Previous approaches results are reported from [26], all based on training from scratch with RGB-only inputs.

Method	Accuracy
I3D [5]	46.5
(2+1)D ResNet-50	46.7
3D ResNet-50	47.9
SlowFast-50 4x4 [12]	48.5
SlowFast-50 8x8 [12]	50.2
SlowFast-101 16x4 [12]	50.8
Backbone (X(2+1)D-M)	48.6
X(2+1)D-M w/ joint space-time module (like [2])	53.3
Ours	<b>53.8</b>

Table 4: Comparison between TokenLearner and the joint space-time transformer modules similar to [2], applied to our backbone. They use the X(2+1)D backbone, tested on Charades with the 6 fps setting, Charades 12 fps setting, and AViD dataset. GFLOPs and # params are of each module (with 64 frame inputs), not the entire network.

Module	Char-6fps	Char-12fps	AViD	GFLOPs	# params
Joint space-time MHSA	57.9	64.0	53.3	22.0	0.30M
Conv2D + Joint space-time MHSA	58.6	62.5	52.5	35.8	1.98M
Ours (TokenLearner)	58.8	63.4	<b>53.8</b>	3.4	0.81M
Ours (Conv2D + TokenLearner)	<b>59.6</b>	<b>66.3</b>	53.7	17.2	2.49M

**Anonymized Videos from Diverse countries (AViD) results:** Table 3 shows the results on the AViD dataset. As seen, our approach outperforms prior work on this challenging dataset too. We also compared ours to the reimplementation of TimeSformer module [3] applied to the same backbone as ours. This uses disjoint spatial and temporal transformer modules, which was also tested in [2].

### 5.3 Ablations

**Comparison against the full space-time transformer:** Here, we compare the TokenLearner against a popular space-time transformer strategy. The full joint space-time transformer module (advocated in [2] and also mentioned in [3]). The full joint space-time transformer module is a single transformer (similar to ours with TokenLearner), but relies only on the hand-designed tokenization. Compared to the TokenLearner which generates  $S * T$  number of tokens, the full joint space-time transformer uses  $H * W * T$  number of tokens. In our case, it uses  $\sim 8$  times more tokens (i.e.,  $8 \times 64$  vs.  $8 \times 8 \times 64$ ). In order to implement these transformer modules, the standard multi-head self-attention (MHSA) [38] with 8 heads is used. This could be viewed as the module identical to [2], except that we follow the bottleneck transformer network design.

Table 4 shows the results. Interestingly, despite the heavier computation of the full joint space-time transformer, it performed worse to the TokenLearner modules. We believe this shows the advantage of the ‘adaptiveness’ of the tokens in the TokenLearner and shows that the standard transformers might be suffering from the tokens irrelevant to the actions serving as noise.

We also report the amount of computation and the number of parameters of each module in these models. This depends on the input size and the hyper parameter setting, and our measurement is based on the input size (i.e.,  $H \times W \times T \times C$ ) of  $8 \times 8 \times 64 \times 492$ . Note that this is the measurement of modules, not the entire network.

**Comparison between multiple space-time layer combinations.** As also suggested in previous literature, it is a common strategy for video representations to pair a layer focusing on spatial information with a layer focusing on temporal information (e.g., R(2+1)D [37] and TimeSformer [3]). Table 5 shows the results of this ablation. For spatial and temporal transformer implementations,

Table 5: Comparison between different space-time transformer modules. They were all applied to the same backbone architecture (i.e., the Bottleneck Transformer-style with X(2+1)D). The Charades-6fps is used in this experiment. FLOPS are estimated with 64-frame settings, per module.

Module	Charades-6fps (%)	GFLOPs	# params
Conv2D + Conv1D	56.6	18.3	2.24M
Conv2D + MLP Mixer [35]	57.0	13.8	2.06M
Conv2D + Temporal transformer	58.4	16.5	1.98M
Spatial + Temporal transformer	58.8	5.5	0.59M
Conv2D + Spatial + Temporal transformer	58.0	19.2	2.27M
Ours (TokenLearner)	58.8	3.4	0.81M
Ours (SpatialT + TokenLearner)	58.9	6.2	1.11M
Ours (Conv2D + TokenLearner)	59.6	17.2	2.49M

Table 6: Comparing different components of our TokenLearner. On Charades dataset (6fps).

Module	Accuracy (%)
Standard transformer (MHSA)	58.4
Vector transformer (VectT)	58.1
Prior-only-attention + broadcasting	58.6
Vector transformer (VectT) + broadcasting	58.9
Vector transformer (VectT) + TokenFuser	59.0
TokenLearner + MHSA + TokenFuser	59.0
TokenLearner + VectT + TokenFuser	59.6

the standard multi-head self-attention was used, as was done in [2, 3]. The result shows that the proposed TokenLearner is more accurate than other popular combinations. The modules based on TokenLearner also effectively only uses a fraction of the Tokens per frame (i.e., 8) as opposed to other methods which use  $16 \times 16$  or  $32 \times 32$  tokens.

our measurement is based on the input size (i.e.,  $H \times W \times T \times C$ ) of  $8 \times 8 \times 64 \times 492$ .

One of the main benefits of the TokenLearner (in addition to the adaptive tokenization of the input and that we explicitly fuse the tokens to capture their spatio-temporal patterns) is that, unlike the disjoint space/time transformers used in this ablation study, it is a joint space-time transformer. Simultaneously, it still manages its computation to be much more tractable (as shown in Table 5): A naive full version of the space-time transformer would require consideration of  $8 \times 8 \times 64 = 4096$  tokens in our case, building and multiply the attention tensor of size  $4096 \times 4096 \times 492$ . On the other hand, the TokenLearner learns to consider  $8 \times 64 = 512$  tokens jointly.

**Different components.** We did an ablation to evaluate components of our adaptive token transformer and their combinations. We conducted ablations removing/adding different components of our model. In addition to the vector transformer described in Section 2, we also tried an ablation of replacing it with the multi-head self-attention. Table 6 shows the results, demonstrating the benefits each of the elements bring to the approach. For this experiment, we used the module composed of Conv2D + transformer, which we found to perform the best from the above ablation.

**TokenLearner alternatives.** We also compared our spatial attention-based token learning with alternative approaches: (1) using a fixed grid to split each frame into the same number of tokens (i.e., 8 tokens), (2) the approach of directly generating tokens using a fully connected layer, and (3) the approach of spatially average pooling the entire frame pixels and using fully connected layers to generate multiple tokens per frame. In the second approach, we directly model  $z_i = A_i(x)$  as a dense layer, producing  $H \times S \times C$  tensor based on the  $H \times W \times T \times C$  input. The third approach is similar, except that we apply spatial global average pooling per frame and then use MLP to generate tokens.

The fixed split tokenization method (1) provided us the accuracy of 58.8 on Charades, as opposed to 59.6 of ours. The direct token generation method (2) provided the accuracy of 56.6 on Charades,

failing to obtain better tokens. Pooling and generation method (3) gave us the accuracy of 58.6. These results suggest the importance of spatial attention for the token learning, our TokenLearner. The same vector transformer and TokenFuser (from Section 2) were used for this ablation.

## 5.4 Visualizations

Figure 8 shows visualizations of the tokens being learned with our approach. We show the spatial attention maps (i.e.,  $\alpha_i(x)$ ) from the first TokenLearner module, as the inputs to the higher-level TokenLearner becomes more mixed spatially and temporally. We are able to observe that they tend to focus more on human regions, and that they change over time responding to the changes in the visual input. Among the  $S = 8$  tokens per frame we learn, we visualize 4 of them.

## 6 Related work

Video understanding relies on both the spatial and the temporal information in the video. In order to adequately capture both motion and appearance information in videos, full 3D space-time convolutional layers as well as (2+1)D convolutional layers have been used [36, 5, 37, 43]. More advanced network designs have also been extremely popular in video CNNs particularly two-stream ones [31, 13, 14, 15, 8, 12] and, recently, architecture searched ones [11, 29, 25].

Attention-based architectures, e.g., the Transformer [38] have shown remarkable success in both Natural Language processing (NLP) and computer vision. Most adaptations of the Transformer architectures to computer vision, have been slow, although some optimizations, have been successful e.g., for image classification, [4, 44, 6, 27] and for video generation [41].

Applying attention-based architectures to video presents a definite challenge as the model needs to learn dependencies across both the spatial and temporal domains. The Vision Transformer [9] demonstrated how the NLP-specific Transformer architecture can elegantly work for images, by subdividing the input image into non-overlapping patches on a regular grid and feeding them as token embeddings to the Transformer, where  $O(N^2)$  tokens are used or order of 256 or 1024. [16] relied on the region proposal network to use the detected human and object candidates as tokens, showing that it could be combined with CNNs.

A couple of recent (unpublished) work [2, 3], in the spirit of the Vision Transformer, subdivided the video into token in a 3D grid to capture the video input. This leads to  $O(N^3)$  increase in the number of tokens required for learning (typically  $\sim 25k$  tokens for 96-frame model). Our work, in contrast, learns the tokens from data which results in a significantly fewer tokens, and more efficient approach. We see that even 8x times fewer tokens (e.g., 512 vs 4096), when learned, are able to capture successfully the information needed for video representation learning.

## 7 Conclusions

We have presented TokenLearner, a novel approach for space-time representation learning in visual data, which adaptively tokenizes the input space. The goal is to learn the important tokens in images and video frames for the recognition tasks at hand. Our approach is more efficient, than contemporary work, by finding few important space-time tokens which can model interactions within images and videos. We observe improved accuracies across image classification and challenging video understanding tasks. One of the remaining challenges is in learning full spatio-temporal tokens. The current TokenLearner focuses on finding spatial tokens over a sequence of frames, and it could be extended to mine tokens over space-time volumes.

## Acknowledgement

We thank Dmitry Kalashnikov, Andy Zeng, and Robotics at Google NYC team members for valuable discussions on attention mechanisms.

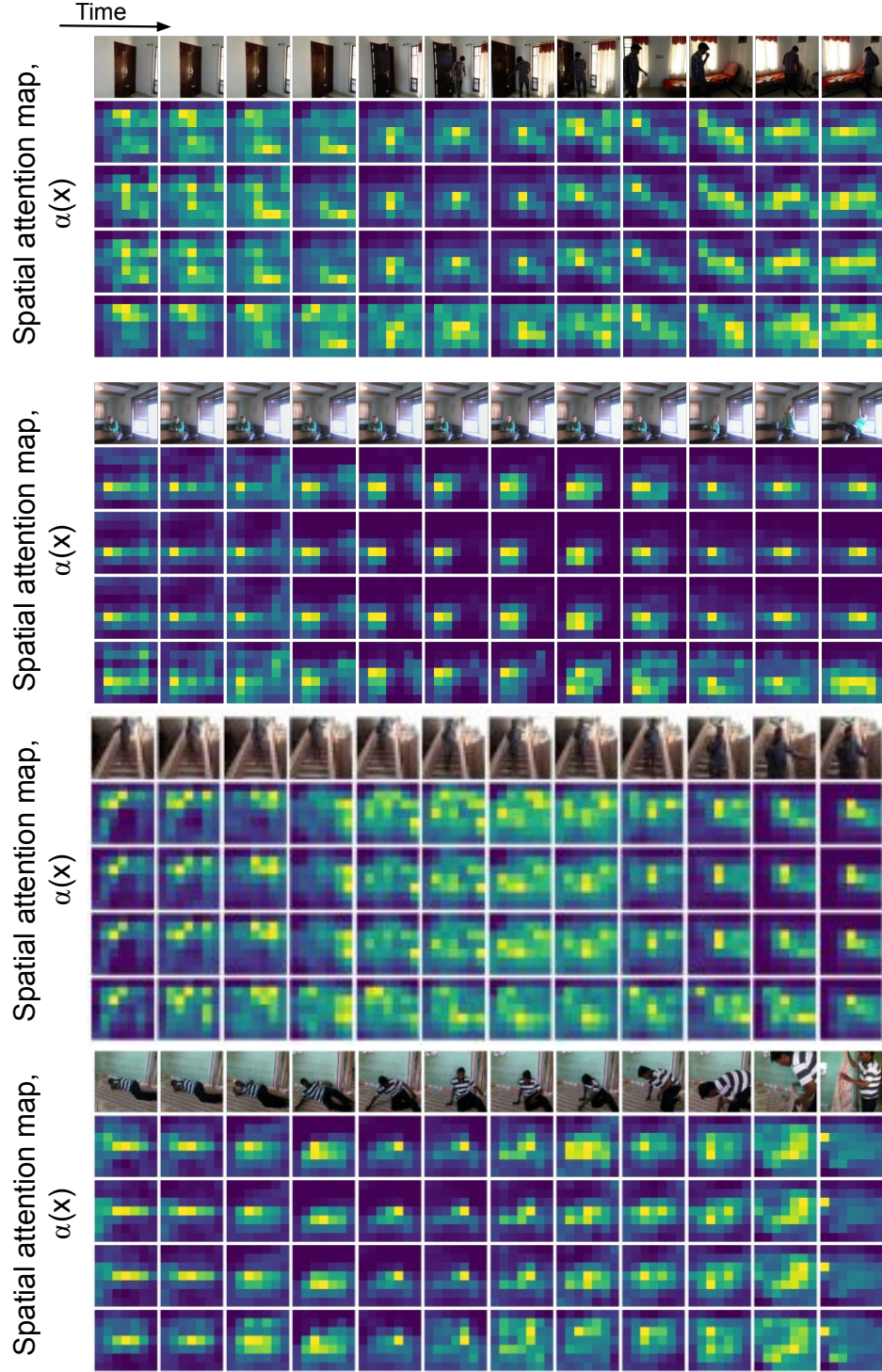


Figure 8: Visualization of the spatial attention maps for the tokenizations. Attention maps for four among a total of eight learned tokens are shown.

## References

- [1] J.-B. Alayrac, A. Recasens, R. Schneider, R. Arandjelović, J. Ramapuram, J. D. Fauw, L. Smaira, S. Dieleman, and A. Zisserman. Self-supervised multimodal versatile networks. In *Advances in Neural Information Processing Systems (NeurIPS)*, 2020.
- [2] A. Arnab, M. Dehghani, G. Heigold, C. Sun, M. Lučić, and C. Schmid. ViViT: A video vision transformer. *arXiv preprint arXiv:2103.15691*, 2021.
- [3] G. Bertasius, H. Wang, and L. Torresani. Is space-time attention all you need for video understanding? *arXiv preprint arXiv:2102.05095*, 2021.
- [4] N. Carion, F. Massa, G. Synnaeve, N. Usunier, A. Kirillov, and S. Zagoruyko. End-to-end object detection with transformers. In *Proceedings of European Conference on Computer Vision (ECCV)*, 2020.
- [5] J. Carreira and A. Zisserman. Quo vadis, action recognition? a new model and the kinetics dataset. In *Proceedings of the IEEE Conference on Computer Vision and Pattern Recognition (CVPR)*, 2017.
- [6] J. Cordonnier, A. Loukas, and M. Jaggi. On the relationship between self-attention and convolutional layers. In *International Conference on Learning Representations (ICLR)*, 2020.
- [7] J. Deng, W. Dong, R. Socher, L.-J. Li, K. Li, and L. Fei-Fei. Imagenet: A large-scale hierarchical image database. In *Proceedings of the IEEE Conference on Computer Vision and Pattern Recognition (CVPR)*, 2009.
- [8] A. Diba, M. Fayyaz, V. Sharma, M. Paluri, J. Gall, , R. Stiefelhagen, and L. V. Gool. Holistic large scale video understanding. *arXiv preprint arXiv:1904.114511*, 2019.
- [9] A. Dosovitskiy, L. Beyer, A. Kolesnikov, D. Weissenborn, X. Zhai, T. Unterthiner, M. Dehghani, M. Minderer, G. Heigold, S. Gelly, J. Uszkoreit, and N. Houlsby. An image is worth 16x16 words: Transformers for image recognition at scale. *arXiv preprint arXiv:2010.11929*, 2020.
- [10] H. Fan, B. Xiong, K. Mangalam, Y. Li, Z. Yan, J. Malik, and C. Feichtenhofer. Multiscale vision transformers. *arXiv preprint arXiv:2104.11227*, 2021.
- [11] C. Feichtenhofer. X3D: expanding architectures for efficient video recognition. In *Proceedings of the IEEE Conference on Computer Vision and Pattern Recognition (CVPR)*, June 2020.
- [12] C. Feichtenhofer, H. Fan, J. Malik, and K. He. Slowfast networks for video recognition. In *Proceedings of the IEEE International Conference on Computer Vision (ICCV)*, 2019.
- [13] C. Feichtenhofer, A. Pinz, and R. Wildes. Spatiotemporal residual networks for video action recognition. In *Advances in Neural Information Processing Systems (NeurIPS)*, pages 3468–3476, 2016.
- [14] C. Feichtenhofer, A. Pinz, and R. P. Wildes. Spatiotemporal multiplier networks for video action recognition. In *Proceedings of the IEEE Conference on Computer Vision and Pattern Recognition (CVPR)*, pages 4768–4777, 2017.
- [15] C. Feichtenhofer, A. Pinz, and A. Zisserman. Convolutional two-stream network fusion for video action recognition. In *Proceedings of the IEEE Conference on Computer Vision and Pattern Recognition (CVPR)*, pages 1933–1941, 2016.
- [16] R. Girdhar, J. Carreira, C. Doersch, and A. Zisserman. Video action transformer network. In *Proceedings of the IEEE Conference on Computer Vision and Pattern Recognition (CVPR)*, 2019.
- [17] K. Hara, H. Kataoka, and Y. Satoh. Learning spatio-temporal features with 3d residual networks for action recognition. In *Proceedings of the ICCV Workshop on Action, Gesture, and Emotion Recognition*, volume 2, page 4, 2017.
- [18] J. Hu, L. Shen, S. Albanie, G. Sun, and E. Wu. Squeeze-and-excitation networks. In *Proceedings of the IEEE Conference on Computer Vision and Pattern Recognition (CVPR)*, 2018.
- [19] J. Ji, R. Krishna, L. Fei-Fei, and J. C. Niebles. Action genome: Actions as composition of spatio-temporal scene graphs. In *Proceedings of the IEEE Conference on Computer Vision and Pattern Recognition (CVPR)*, 2020.
- [20] S. Ji, W. Xu, M. Yang, and K. Yu. 3d convolutional neural networks for human action recognition. *IEEE Transactions on Pattern Analysis and Machine Intelligence*, 35(1):221–231, 2013.
- [21] W. Kay, J. Carreira, K. Simonyan, B. Zhang, C. Hillier, S. Vijayanarasimhan, F. Viola, T. Green, T. Back, P. Natsev, et al. The kinetics human action video dataset. *arXiv preprint arXiv:1705.06950*, 2017.
- [22] D. Kondratyuk, L. Yuan, Y. Li, L. Zhang, M. Tan, M. Brown, and B. Gong. Movinets: Mobile video networks for efficient video recognition. In *Proceedings of the IEEE Conference on Computer Vision and Pattern Recognition (CVPR)*, 2021.
- [23] M. Monfort, A. Andonian, B. Zhou, K. Ramakrishnan, S. A. Bargal, T. Yan, L. Brown, Q. Fan, D. Gutfrund, C. Vondrick, et al. Moments in time dataset: one million videos for event understanding. *arXiv preprint arXiv:1801.03150*, 2018.

- [24] A. Piergiovanni, A. Angelova, and M. S. Ryoo. Evolving losses for unsupervised video representation learning. 2020.
- [25] A. Piergiovanni, A. Angelova, A. Toshev, and M. S. Ryoo. Evolving space-time neural architectures for videos. *Proceedings of the IEEE International Conference on Computer Vision (ICCV)*, 2019.
- [26] A. Piergiovanni and M. S. Ryoo. AViD dataset: Anonymized videos from diverse countries. In *Advances in Neural Information Processing Systems (NeurIPS)*, 2020.
- [27] P. Ramachandran, N. Parmar, A. Vaswani, I. Bello, A. Levskaya, and J. Shlens. Stand-alone self-attention in vision models. In *Advances in Neural Information Processing Systems (NeurIPS)*, 2019.
- [28] M. S. Ryoo, A. Piergiovanni, J. Kangaspunta, and A. Angelova. AssembleNet++: Assembling modality representations via attention connections. In *Proceedings of European Conference on Computer Vision (ECCV)*, 2020.
- [29] M. S. Ryoo, A. Piergiovanni, M. Tan, and A. Angelova. AssembleNet: Searching for multi-stream neural connectivity in video architectures. In *International Conference on Learning Representations (ICLR)*, 2020.
- [30] G. A. Sigurdsson, G. Varol, X. Wang, A. Farhadi, I. Laptev, and A. Gupta. Hollywood in homes: Crowdsourcing data collection for activity understanding. In *Proceedings of European Conference on Computer Vision (ECCV)*, 2016.
- [31] K. Simonyan and A. Zisserman. Two-stream convolutional networks for action recognition in videos. In *Advances in Neural Information Processing Systems (NeurIPS)*, pages 568–576, 2014.
- [32] A. Srinivas, T. Lin, N. Parmar, J. Shlens, P. Abbeel, and A. Vaswani. Bottleneck transformers for visual recognition. *arXiv preprint arXiv:2101.11605*, 2021.
- [33] J. C. Stroud, D. A. Ross, C. Sun, J. Deng, and R. Sukthankar. D3D: Distilled 3d networks for video action recognition. *arXiv preprint arXiv:1812.08249*, 2018.
- [34] C. Sun, A. Shrivastava, S. Singh, and A. Gupta. Revisiting unreasonable effectiveness of data in deep learning era. In *Proceedings of the IEEE International Conference on Computer Vision (ICCV)*, 2017.
- [35] I. Tolstikhin, N. Houlsby, A. Kolesnikov, L. Beyer, X. Zhai, T. Unterthiner, J. Yung, A. Steiner, D. Keysers, J. Uszkoreit, M. Lucic, and A. Dosovitskiy. Mlp-mixer: An all-mlp architecture for vision. *arXiv preprint arXiv:2105.01601*, 2021.
- [36] D. Tran, L. D. Bourdev, R. Fergus, L. Torresani, and M. Paluri. C3d: generic features for video analysis. *CoRR, abs/1412.0767*, 2(7):8, 2014.
- [37] D. Tran, H. Wang, L. Torresani, J. Ray, Y. LeCun, and M. Paluri. A closer look at spatiotemporal convolutions for action recognition. In *Proceedings of the IEEE Conference on Computer Vision and Pattern Recognition (CVPR)*, pages 6450–6459, 2018.
- [38] A. Vaswani, N. Shazeer, N. Parmar, J. Uszkoreit, L. Jones, A. N. Gomez, L. Kaiser, and I. Polosukhin. Attention is all you need. In *Advances in Neural Information Processing Systems (NeurIPS)*, 2017.
- [39] X. Wang, R. Girshick, A. Gupta, and K. He. Non-local neural networks. In *Proceedings of the IEEE Conference on Computer Vision and Pattern Recognition (CVPR)*, pages 7794–7803, 2018.
- [40] X. Wang and A. Gupta. Videos as space-time region graphs. In *Proceedings of European Conference on Computer Vision (ECCV)*, pages 399–417, 2018.
- [41] D. Weissenborn, O. Täckström, and J. Uszkoreit. Scaling autoregressive video models. In *International Conference on Learning Representations (ICLR)*, 2020.
- [42] C.-Y. Wu, C. Feichtenhofer, H. Fan, K. He, P. Krähenbühl, and R. Girshick. Long-term feature banks for detailed video understanding. *arXiv preprint arXiv:1812.05038*, 2018.
- [43] S. Xie, C. Sun, J. Huang, Z. Tu, and K. Murphy. Rethinking spatiotemporal feature learning: Speed-accuracy trade-offs in video classification. In *Proceedings of European Conference on Computer Vision (ECCV)*, pages 305–321, 2018.
- [44] H. Zhao, J. Jia, and V. Koltun. Exploring self-attention for image recognition. In *Proceedings of the IEEE Conference on Computer Vision and Pattern Recognition (CVPR)*, June 2020.

## **A Appendix**

### **A.1 Image classification training details**

We follow the exact training protocols and the hyper parameters of [9] for our image classification experiments.

### **A.2 Video classification training details**

We provide the training details as below. For the training/testing splits of the datasets, we followed their standard settings.

We use the cosine-decay learning rate which was popularly used in many video CNN model trainings. The base learning rate of 0.8 per TPU core (which is equivalent to a single GPU) is used for the Charades dataset (multi-label action classification) and the base rate of 0.025 per TPU was used for the AViD dataset (video classification). The training was done for 100k iterations with the batch size of 4 per TPU core (i.e.,  $4 \times 64 = 256$  was our batch size) in the Charades experiments. The batch size of 8 per TPU core was used for AViD. 100k iterations correspond to roughly 125 epoches in AViD. Label smoothing of 0.2 was used for the AViD training. No label smoothing was used for the Charades. In Charades, the training was done by temporally cropping a long Charades videos (e.g., 30 seconds) into 64 frame segments. The evaluation was done similarly with 64 frame segments by merging their output responses.

The training time of a single model was around  $\sim 16$  hours with 32 TPU v3. This was bottlenecked by the data pipeline, and the actual computation is less.